第 34 卷第 4 期
2018 年 4 月

无 机 化 学 学 报
CHINESE JOURNAL OF INORGANIC CHEMISTRY

Vol.34 No.4
750-756

钠离子电池正极材料 $NaNi_{1/3}Co_{1/3}Mn_{1/3}O_2$ 高压衰减机理

王 勇[1] 刘 雯[1] 郭 瑞[1] 罗 英[2] 李 永[1] 裴海娟[1] 解晶莹*,[1,2]

([1]上海空间电源研究所,空间电源技术国家重点实验室,上海 200245)

([2]上海动力储能电池系统工程技术有限公司,上海 200241)

摘要：首次通过简单的固相反应合成了 $NaNi_{1/3}Co_{1/3}Mn_{1/3}O_2$ 材料,并对其合适的电化学工作条件进行了探索。在此基础上对其在高充电电压下的衰减机理进行了研究。通过非原位 XRD 和电化学阻抗谱等电化学手段综合分析高充电电压下的衰减机理,发现随着充电电压升高至 4 V,界面层的不断增厚与材料结构的不可逆变化同时导致了电化学性能的衰减。

关键词：钠离子电池；正极材料；机理；容量衰减；高充电电压

中图分类号：O614.81+3；O614.81+2；O614.7+11　　**文献标识码**：A　　**文章编号**：1001-4861(2018)04-0750-07

DOI:10.11862/CJIC.2018.074

Mechanism on Capacity Fading at Higher Charging Potential of $NaNi_{1/3}Co_{1/3}Mn_{1/3}O_2$ for Sodium Ion Batteries

WANG Yong[1] LIU Wen[1] GUO Rui[1] LUO Ying[2] LI Yong[1] PEI Hai-Juan[1] XIE Jing-Ying*,[1,2]

([1]*State Key Laboratory of Space Power-Sources Technology, Shanghai Institute of Space Power-Sources, Shanghai* 200245, *China*)

([2]*Shanghai Power Energy Storage Battery System Engineering Technology Co., Ltd., Shanghai* 200241, *China*)

Abstract: $NaNi_{1/3}Co_{1/3}Mn_{1/3}O_2$ material was synthesized by a facile method, and the suitable working voltages (3.75 V, 4 V) are investigated afterwards. The mechanisms of capacity fading when charging to 4 V are studied by *ex-situ* XRD and EIS measurements, which revealed a collective effect between the thicker of the SEI layer and the irreversible variation of the material structure.

Keywords: sodium ion battery; cathode material; mechanism; capacity fading; high charge voltage

0 Introduction

Due to the abundance and relatively low cost of sodium-containing resources, the development of the sodium ion battery is rapidly growing[1-2]. However, the lack of high performance cathodes still prevents the commercialization of sodium ion battery. Among the cathode materials of sodium ion battery, O3 type layered oxides $NaMO_2$ (M=metals, such as Ni, Co, Mn, Ti, Fe, Cr and so on[3-8]) have been widely investigated because of their high specific capacity and good cyclic retention[9-13]. During the investigation of transition layered oxides, many materials have shown good cyclic performance or specific capacity. For example, $NaNi_{1/2}Mn_{1/2}O_2$ delivers a reversible capacity of 125 $mAh\cdot g^{-1}$ [14] with over 90% capacity retention after 50 cycles, whereas $Na(FeCrMn)_{1/3}O_2$ exhibits an initial capacity of 186 $mAh\cdot g^{-1}$ [15] with 50% capacity retention after 30 cycles. For one given material, a wider voltage range often means a larger capacity. Also, a higher charge voltage is pursued for a larger specific energy density. However, different voltage range would affect

收稿日期:2017-10-23。收修改稿日期:2017-12-17。

国家自然科学基金(No.21373137)、国家 863 项目(No.2014AA052202)和上海市自然科学基金(No.15DZ2282000)资助。

*通信联系人。E-mail:jyxie@mail.sim.ac.cn

significantly upon the properties during the charge/discharge process, which mainly caused by the different ratio of Na^+ extraction/insertion from the structure. As a classical cathode material, O3-type $NaFeO_2$ can deliver 80~100 mAh·g^{-1} of reversible capacity when charging to different potential. When charging to 3.40 V, 0.30 mol Na^+ can be extracted from the structure, accompanying with 80 mAh·g^{-1} of discharge capacity. When charging to 3.50 V, approximately 0.45 Na^+ can be extracted from the structure, accompanying with 110 mAh·g^{-1} of discharge capacity[16]. But with the increasing charge voltage afterwards, the capacity fades fast, it could only deliver ~30 mAh·g^{-1} of discharge capacity when charging to 4.50 V. Similarly, $NaNi_{0.5}Mn_{0.5}O_2$ material owns 120 mAh·g^{-1} reversible capacity and a good capacity retention at the potential range of 2~3.80 V. However, it shows poor capacity retention when charging to 4.50 V [14]. Therefore, a suitable working voltage is quite important for a better electrochemical behavior.

Similar to $LiNi_{1/3}Co_{1/3}Mn_{1/3}O_2$ in lithium ion battery, $NaNi_{1/3}Co_{1/3}Mn_{1/3}O_2$ material is an attractive cathode for sodium ion battery. Prakash et al.[17] have successfully prepared $NaNi_{1/3}Co_{1/3}Mn_{1/3}O_2$ by sol-gel method using corresponding acetates, which shows a capacity of 120 mAh·g^{-1} between 2~3.75 V at the rate of 0.10C. After 50 cycles, the capacity retention is about 93%, which has superiority over the other layered oxide materials. In previous work, sol-gel method is applied to manufacture the O3 type $NaNi_{1/3}Co_{1/3}Mn_{1/3}O_2$ material, which is not suitable for the application when it comes to industrial scale. Comparing to the sol-gel preparation process, solid-state reaction owns more convenience and lower costs with little waste during the production process, which means that solid-state reaction would possibly be a feasible way for a material preparation at industrial scale.

In this work, a facile method to prepare $NaNi_{1/3}Co_{1/3}Mn_{1/3}O_2$ (denoted as NNCM-333) was studied. Using a solid-state reaction, $NaNi_{1/3}Co_{1/3}Mn_{1/3}O_2$ had been successfully prepared, and its electrochemical performances were tested. This material exhibits an initial discharge capacity of 120 mAh·g^{-1} and a capacity retention of 93% after 50 cycles at a rate of 0.10C at the potential range of 2~3.75 V. A comprehensive study for an optimized working voltage has been investigated. A possible mechanism for the capacity fade when working at the potential of 2~4 V is proposed.

1　Experimental

1.1　Material synthesis

$NaNi_{1/3}Co_{1/3}Mn_{1/3}O_2$ material is synthesized via a conventional solid-state reaction. Na_2CO_3, NiO, Co_2O_3, MnO_2 are mixed with respective mole ratio and then pressed into pellets. The precursors are sintered at 900 ℃ for 12 hours, and then cooled to room temperature at atomsphere.

1.2　Material characterization

The morphology of the product is characterized by field emission scanning electron microscopy (FE-SEM, Hitachi S-4800) operated at an accelerating voltage of 10 kV. High resolution transmission electron microscopy (HRTEM) and select-area electron diffraction (SAED) are examined for the structure of the as-prepared sample operated at an accelerating voltage of 200 kV. Powder X-ray diffraction (XRD) patterns are collected on an X-ray diffractometer (Bruker D8 Advance, Germany) with Cu $K\alpha$ radiation (λ=0.154 18 nm) at 40 kV, 40 mA. Data are obtained over the 2θ= 10°~90° with a scan rate of 1°·min^{-1}.

1.3　Electrochemical characterization

The working electrodes are composed of NNCM-333, Super P and polyvinylidenefluoride (PVDF) with a mass ratio of 7∶2∶1 on aluminum foil. The loading amount of active materials is about 1 mg·cm^{-2}. Coin cells (CR2016) are assembled in an Ar-filled glovebox. 0.90 mol·L^{-1} $NaPF_6$ in the non-aqueous solution of 1,2-dimethoxyethane (DME) is used as electrolyte. A glass-fiber (Whatman GF/F) is used as the separator and pure sodium foil is used as the counter electrode (anode). Galvanostatic charge-discharge measurements are carried out at 25 ℃ with a LAND battery test system. And the current density is calculated on the basis of the specific capacity and the weight of active

material. The cyclic voltammetry tests are carried out at 25 ℃ with a Princeton Applied Research electrochemical workstation at the scan rate of 0.10 mV·s^{-1}.

2 Results and discussion

2.1 Morphology and structure characterization

The crystalline structure is analyzed using XRD, as shown in Fig.1a. All peaks can be well indexed to the hexagonal phase, which refer to a space group of $R\bar{3}m$ and is consistent with the standard literature[17] (PDF No.00-032-1068). This indicates that the single phase O3 type NNCM-333 is synthesized. The lattice parameters are listed as follows: a=0.297 02 nm, b=0.297 02 nm, c=1.683 80 nm; α=90°, β=90°, γ=120°. As we all known that the NNCM-333 material is unstable in air, accompanying with the structural transition from rhombohedral to monoclinic, which always associated with the gliding of $Ni_{1/3}Co_{1/3}Mn_{1/3}O_2$ slabs[18]. SEM image shows that the average particle size of the material is about 20~30 μm. For further characterizing the structure of the NNCM-333 sample, HRTEM and SAED tests are carried out, which are listed in Fig.1(c~d). The SAED image shows a lattice structure that indicates a hexagonal symmetry. In Fig. 1d, the TEM image is observed from [100] direction, which is favorable for Na^+ insertion and extraction. The d-spacing is 0.20 nm.

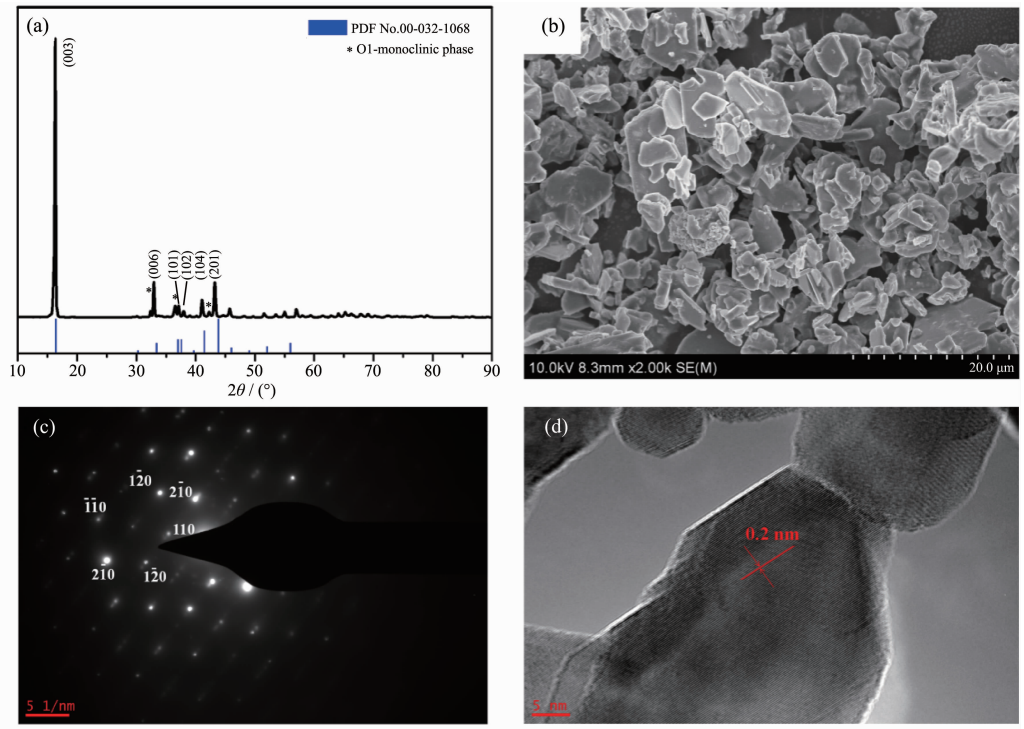

Fig.1 (a) XRD pattern; (b) SEM image; (c) SAED pattern and (d) HRTEM image of as-prepared NNCM-333

2.2 Investigation of working potential

Na/NNCM-333 cells are charging to different charge voltages of 3.75, 4, 4.25 and 4.50 V. Fig.2 (a~b) depicts the first two charge-discharge curves. The open circuit voltage (OCV) lies close to 2.60 V. In the 1st charge process, an obvious plateau is observed between 2.50 and 2.60 V firstly, followed by a sloping voltage plateau to 3.30 V. Another plateau occurs at the potential range of 3.50~3.60 V. When charging over 3.80 V, a plateau between 3.80~4 V is observed. With the cell charging to 4.50 V, a persistent plateau appears close to 4.50 V. In the following discharge process, a symmetrically corresponding curve is observed, expcept for charging to 4.50 V. The electrolyte ($NaPF_6$ in DME) is stable below the voltage of 4.40 V[19]. It would be decomposed at the voltage of 4.50 V. This may be the main reason for the bad electrochemical property when charging to 4.50 V. Furthermore, there is severe capacity fade during the first two cycles when being charged to 4.25 V and

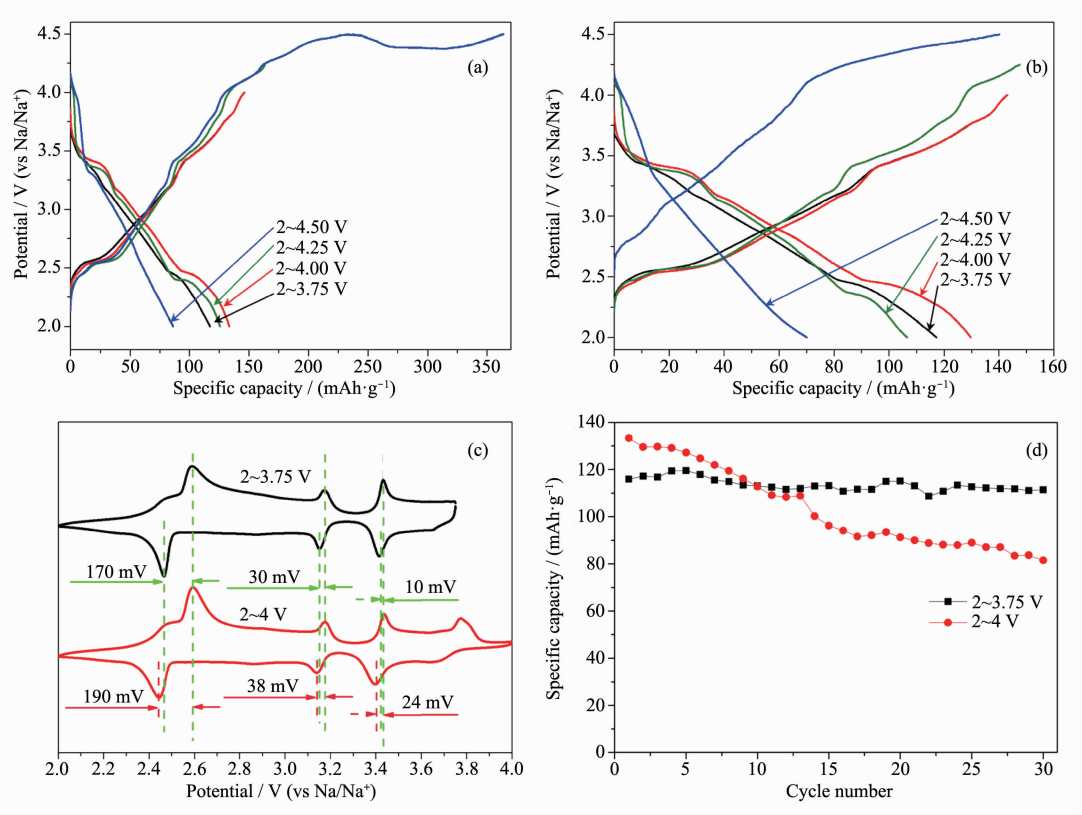

Fig.2　(a) First and (b) 2nd charge-discharge curves with different charge voltage of NNCM-333 sample; (c) CV curves and (d) cyclic performance of NNCM-333 at different potential ranges

4.50 V. Therefore, NNCM-333 cells are cycled at the potential range of 2~3.75 V and 2~4 V below.

Fig.2c show the CV curves of NNCM-333 in the potential range of 2~3.75 V and 2~4 V at a scan rate of 0.10 $mV \cdot s^{-1}$, respectively. There are three cathodic peaks located at 2.65, 3.15 and 3.45 V in the charge process when charging to 3.75 V, and an additional peaks at 3.76 V when charging to 4 V. Conversely, symmetrically corresponding anodic peaks are observed for the next discharge process. A larger polarization of the cathodic and anodic peaks is observed at the potential range of 2~4 V. Na/NNCM-333 cell working in the potential range of 2~4 V shows worse cyclic (57% of initial capacity after 30 cycles) performance than that in 2~3.75 V (97% of initial capacity after 30 cycles), as shown as Fig.2d.

The possible reasons for the capacity fading when charging to 4 V may be listed as following:

(i) When charging to 4 V, the structure of the material may be destroyed, and in the following process of discharging, it cannot release the capacity acquired during the charge process. This could be confirmed by comparing the structure of the pristine and cycled materials, respectively, using ex-situ XRD.

(ii) When charging to 4 V, the solid electrolyte interface (SEI) layer might be thicker than when charged to 3.75 V. This would increase the impedance between the active material and the current collector, which could be identified using an EIS measurement.

To investigate structural variation during the charge/discharge process, *ex-situ* XRD tests are performed after 0 (pristine material), 50 and 100 cycles when working in the range of 2~3.75 V and after 30 cycles when working at the potential range of 2~4 V, respectively, as shown in Fig.3(a~b). (When the material cycling at the potential range of 2~4 V, the cell comes to the termination of life after 30 cycles.) The peaks labled as star (*) are assigned to Al current collector. Corrsponding Rietveld refinements are listed in the Table S1. When working in the range of 2~3.75 V (Fig.3a), it is clearly shown that the phase varied from O3 to O1 during the charge/discharge process,

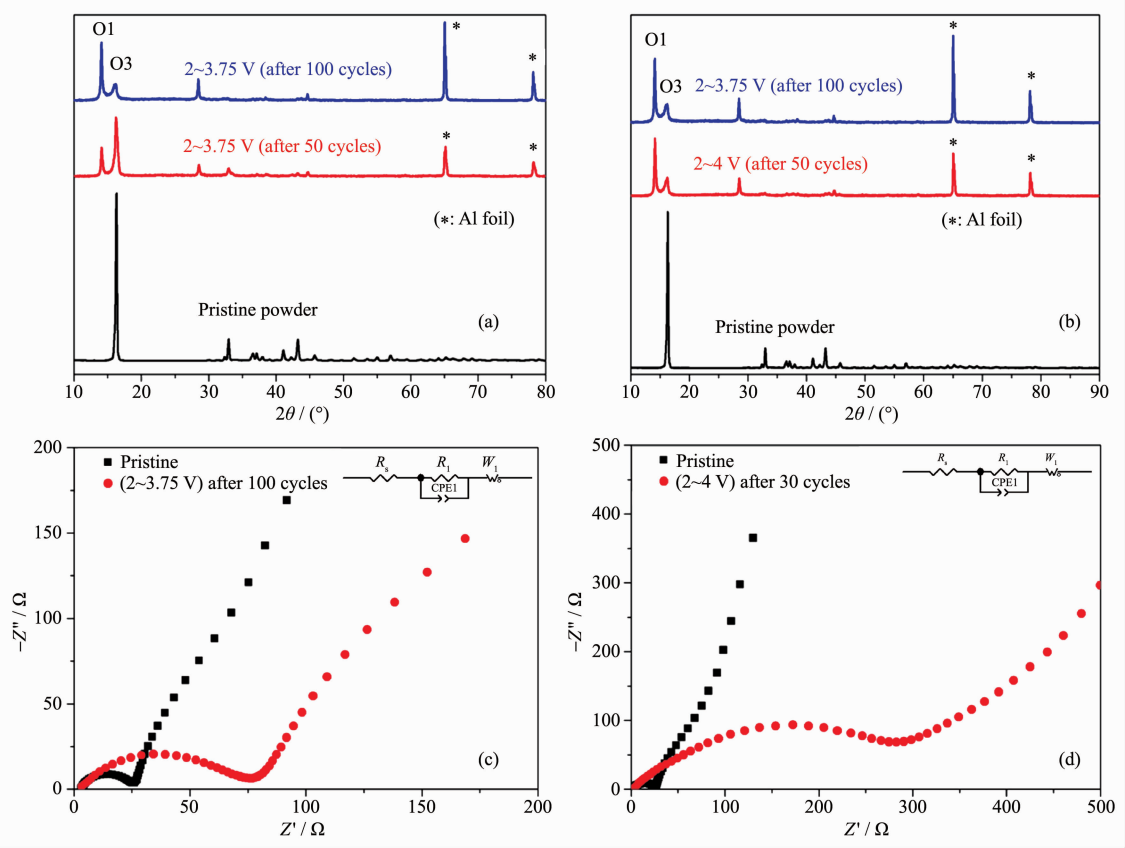

Fig.3 (a) XRD patterns of the pristine material and the NNCM-333 electrodes after 50 and 100 cycles in a voltage range of 2~3.75 V; (b) XRD patterns of the electrode after 30 cycles in a voltage range of 2~4 V and that after 100 cycles in a voltage range of 2~3.75 V for comparison; EIS measurements during cycles at the potential range of (c) 2~3.75 V and (d) 2~4 V (with the insets are the equivalent circuits)

which possibly causes most of the irreversible loss of capacity during the cycle. After 30 cycles in the range 2~4 V (Fig.3b), the structure is almost identical to that after 100 cycles in the range 2~3.75 V, which indicates that the phase variation is accelerated when charging to a higher voltage. After this, the assumption (i) may be reasonably explained.

EIS curves during cycles at the potential range of 2~3.75 V (Fig.3c) and 2~4 V (Fig.3d) indicate the variation of the SEI layer. A proposed equivalent circuit comprising of resistors (R_1), constant phase elements (CPE) and Warburg element (W_1) is listed in the inset of Fig.3(c~d). In Fig.3(c~d), a gap is observed between zero point and the start point, which indicates the negligible solution resistance (R_s). The R_1 refers to the resisitance of the interface of the active material with the current collector, which is gradually larger along with the cycles at the potential range of 2~3.75 V, as shown in Fig.3c, which reveals a thicker SEI layer. Similarly as the structural variation, when the cell comes to the end of life after 30 cycles at the potential of 2~4 V, the increase of the impendence is much more aggravated than that at 2~3.75 V[20].

As mentioned above, it could be summarized that a higher charge potential may acclerate the structural aging of the NNCM-333 material and aggravate the thickness increase of the SEI layer, which would result in the fade of the capacity and the increase of the resistence.

2.3 Electrochemical properties

Considering the poor electrochemical properties at the potential range of 2 ~4 V, the long cycle performance and rate capability are examined under the potential range of 2~3.75 V. Galvanostatic charge-discharge measurements are performed to test the electrochemical properties of NNCM-333. Shown as

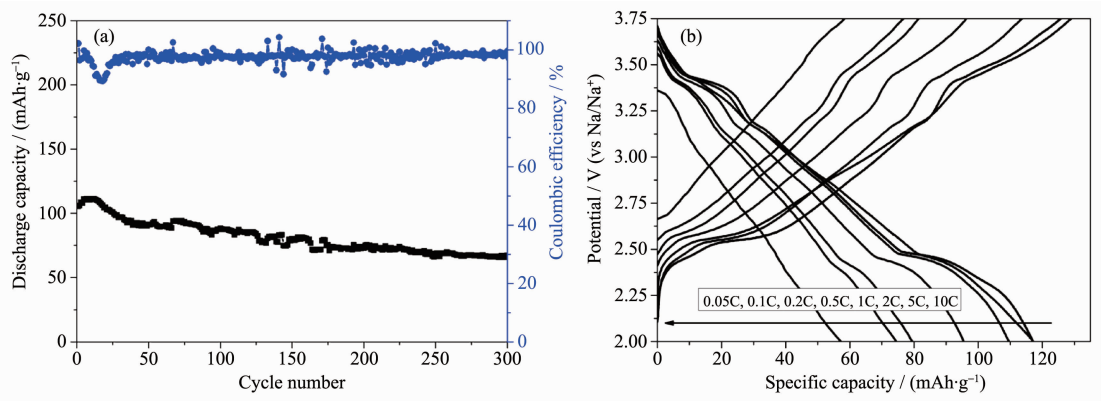

Fig.4　(a) Long cycle performance of the NNCM-333 in the potential range of 2~3.75 V at 0.20C; (b) Second charge-discharge curves of the NNCM-333 at different rates

Fig.S1, the potential-capacity curves show that the electrode yields a 2nd discharge capacity of 118.0 mAh·g^{-1} at the rate of 0.10C. With further cycling, the capacity fades slowly and the polarization becomes larger gradually. The long cycle performance is tested at the rate of 0.20C, depicted as Fig.4a. The sloping increase in the first 10 cycles indicates an activation of the NNCM-333 electrode. NNCM-333 shows a good capacity retention and coulombic efficiency for the first 50 cycles. However, the capacity fades over the subsequent cycles, trending to a stable capacity of 70 mAh·g^{-1}. After 300 cycles, the NNCM-333 holds 60% of the initial capacity. The rate performance is examined of 0.10C, 0.20C, 0.50C, 1C, 2C and 5C, shown as Fig.4b and Fig.S2. The discharge capacity of the NNCM-333 electrode is approximately 60 mAh·g^{-1} even at the rate of 5C. Also, it shows a good rate retention when transferring from 2C to 0.10C after cycling.

3　Conclusions

In summary, a stable O3-$NaNi_{1/3}Co_{1/3}Mn_{1/3}O_2$ is synthesized via solid-state reaction for sodium ion batteries. To find a possible reason for capacity fading when charging to higher potential, a seriel of experiments are tested to confirm the structural and resistance variation between the charge/discharge processes. It is concluded that a higher charge voltage could accelerate the irreversible structure changes and aggravate the increase of SEI layer thickness, which will finally cause the capacity fade. A proper working voltage of 2~3.75 V is settled and the O3-$NaNi_{1/3}Co_{1/3}Mn_{1/3}O_2$ could deliver a reversible capacity of 118 mAh·g^{-1} and over 60% capacity retention after 300 cycles at 0.20C. The O3-$NaNi_{1/3}Co_{1/3}Mn_{1/3}O_2$ has the potential to be a cathode material for energy storage device. With this facile and inexpensive synthesis method, large-scale and room-temperature sodium ion batteries could be more easily commercialized.

Acknowledgments: This work is financially supported by Natural Science Foundation of China (Grant No.21373137), National 863 Program (Grant No.2014AA052202) and Shanghai Science and Technology Development Funds (Grant No. 15DZ2282000).

Supporting information is available at http://www.wjhxxb.cn

References:

[1] Yabuuchi N, Kubota K, Dahbi M, et al. *Chem. Rev.*, **2014**, **114**:11636-11647

[2] Kundu D, Talaie E, Duffort V, et al. *Angew. Chem. Int. Ed.*, **2015**,**54**:3431-3437

[3] Li Y, Yang Z, Xu S, et al. *Adv. Sci.*, **2015**,**2**:1-7

[4] Mu L, Xu S, Li Y, et al. *Adv. Mater.*, **2015**,**27**:6928-6933

[5] FANG Yong-Jin(方永进), CHEN Chong-Xue(陈重学), AI Xin-Ping(艾新平), et al. *Acta Phys.-Chim. Sin.*(物理化学学报), **2017**,**33**:211-241

[6] MU Lin-Qin(穆林沁), QI Xin-Guo(戚兴国), HU Yong-Sheng(胡勇胜), et al. *Energy Storage Sci. Technol.*(储能科学与技术), **2016**,**5**:228-232

[7] Kubotu K, Yabuuchi N, Yoshida H, et al. *MRS Bull.*, **2014**, **39**:416-422

[8] Han M, Conzalo E, Singh G, et al. *Energy Environ. Sci.*, **2015**, **8**:81-102

[9] Yoshida H, Yabuuchi N, Komaba S. *Electrochem. Commun.*, **2013**,**34**:60-63

[10]Kim D, Lee E, Slater M, et al. *Electrochem. Commun.*, **2012**, **18**:66-69

[11]Vassilaras P, Toumar A, Ceder G. *Electrochem. Commun.*, **2014**,**38**:79-81

[12]Yabuuchi N, Kajiyama M, Iwatate J, et al. *Nat. Mater.*, **2012**, **11**:512-517

[13]Yao H R, Wang P F, Wang Y, et al. *Adv. Energy Mater.*, **2017**,**7**:1700189(6 pages)

[14]Komaba S, Nakayama T, Ogata A, et al. *ECS Trans.*, **2009**,**16**: 43-45

[15]Cao M, Wang Y, Shadike Z, et al. *J. Mater. Chem. A*, **2017**, **5**:5442-5447

[16]Sathiya M, Hemalatha K, Ramesha K, et al. *Chem. Mater.*, **2012**,**24**:1846-1848

[17]Yabuuchi N, Yoshida H, Komaba S. *Electrochem.*, **2012**,**80**: 716-719

[18]Hamani D, Ati M, Tarascon J, et al. *Electrochem. Commun.*, **2011**,**13**:938-941

[19]Liu W, Li H, Xie J, et al. *ACS Appl. Mater. Interfaces*, **2014**,**6**:2209-2213

[20]Luo Y, Lu T, Zhang Y, et al. *J. Alloys Compd.*, **2017**,**703**: 289-297